

Use of iron oxide nanomaterials as adsorbents for wastewater treatment

Amira Fadia GHOMRANI^{*}, Sihem ARRIS², Tidjani Ahmed ZITOUNI³

¹Process Engineering Department, Faculty of Science and Technology, Physics of Matter and Radiation Laboratory (LPMR), Mohamed Cherif Messaadia University, BP 1553, 41000 Souk-Ahras, Algeria.

²Environmental Process Engineering Department, Faculty of Process Engineering, Laboratory of Excellence in Engineering and Environmental Processes (LIPE-TAMAYOUZ), Salah Bounider University Constantine 3, Constantine, Algeria

³Mechanical Engineering Department, Mechanical Engineering Laboratory, Faculty of Technical Sciences, Badji Mokhtar Annaba-University (UBMA), Algeria.

Email of the corresponding author ^{*}(a.ghomrani@univ-soukahras.dz)

(Received: 05 June 2023, Accepted: 20 June 2023)

(1st International Conference on Pioneer and Innovative Studies ICPIS 2023, June 5-7, 2023)

ATIF/REFERENCE: Ghomrani, A. F., Arris, S. & Zitouni, T. A. (2023). Use of iron oxide nanomaterials as adsorbents for wastewater treatment. *International Journal of Advanced Natural Sciences and Engineering Researches*, 7(5), 45-50.

Abstract – The dissemination of chemical components into the environment might provoke harm to human health, animal species and the ecosystem. In order to reduce the negative effects of those pollutants, physico-chemical treatment procedures, namely the adsorption technique has been implemented. This study seeks to synthesize manufactured nanomaterials throughout a co-precipitation process such as nanoparticles (Ferrihydrite (Fh)) and nanocomposite magnetic iron (magnetite / activated carbon) capable of adsorbing certain inorganic species (heavy metals) such as hexavalent chromium Cr (VI). The prepared supports were characterized by IRTF analysis. The influence of the various experimental parameters (the initial concentration and the contact time) have been studied. Various isothermal models have been applied, namely Langmuir, Freundlich, Temkin and BET. The study of those absorption isotherms has shown that Langmuir's model describes better Cr (VI) adsorption. It has been also noticed that the adsorption process on the Fh follows a pseudo 2nd order kinetics for the hexavalent chromium. The experimental results have proved that equilibrium is reached after 15 minutes with a better yield of 99.511% and a maximum retention capacity of 40.9157 mg / g.

Keywords – Ferrihydrite (Fh); Magnetite; Manufactured Nanomaterials; Nanocomposite; Co-Precipitation; Isotherm

I. INTRODUCTION

The release of chemical compounds into the environment can cause damage to human health, animal species and the ecosystem. In order to reduce the negative effects of these pollutants, physico-chemical treatment procedures, including the adsorption technique, have been implemented [1]. This study aims at synthesizing engineered nanomaterials through a co-precipitation process namely; Ferrihydrite (Fh) nanoparticles and magnetic iron nanocomposites (magnetite/activated

carbon) capable of adsorbing heavy metals such as hexavalent chromium Cr (VI).

II. MATERIALS AND METHOD

The approach that we followed was to test the adsorption capacity and effectiveness of particles (Ferrihydrite) for the elimination and depollution of industrial effluent containing metallic inorganic pollutants (Cr (VI)). The current study is organized around two main points:

- Chemical co-precipitation is used to synthesize adsorbents, which are manufactured nanoparticles such as ferrihydrite and composite materials based on iron oxide and industrial activated carbon. Then, they were characterized by IRTF analysis.

- Evaluation of adsorption experiments (UV-Visible spectrophotometric dose) of the mineral contaminant hexavalent chromium on synthetic ferrihydrite powder and composite material.

III. RESULTS

1 ANALYSIS BY IRTF SPECTROSCOPY

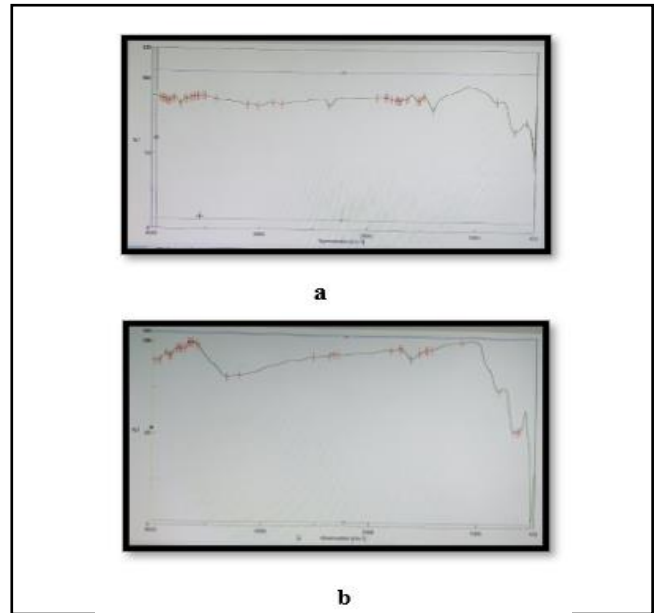


Fig. 2 IR spectrum of the synthesized Ferrihydrite (Fh) before (a) and after adsorption (b)

Table 1. Main detected groups of Fh before adsorption

Wave number (cm ⁻¹)	Bonds	Nature of the vibration
3416.28	O-H or N-H	Elongation (stretching) vibration of the hydroxyl groups (alcohol) of the O-H bonds or with the N-H amine groups [2], [3], [4].
1626.66	H ₂ O	Water molecules adsorbed on nanoparticles [5], [6], [7].
1531.20 and 1481.06	Fe-O	Vibration band corresponding to the deformation (bending) of Fe-O links [7], [6].
1400.07	Fe-OH	Vibration band corresponding to the deformation of Fe-OH bonds [6], [7], [8].

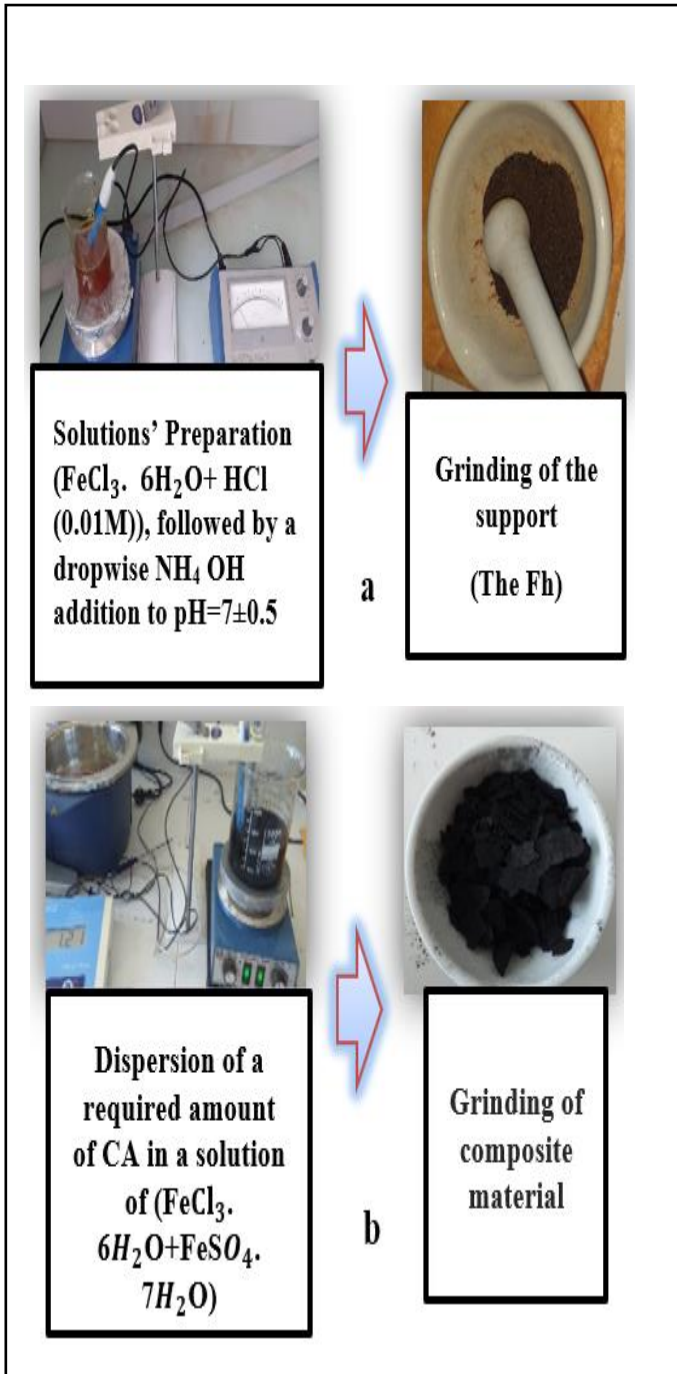


Fig. 1 Synthesis of iron oxide nanoparticles a) Ferrihydrite (Fh); b) Nanocomposite (Magnetite/Active Carbon (CA))

Table 2. Main detected groups of Fh after adsorption

Wave number (cm ⁻¹)	Bonds	Nature of the vibration
3582.13 (Very wide)	O-H or N-H	The absorption band is probably associated with the elongation (stretching) vibration of the hydroxyl groups (alcohol) of the O-H bonds or with the N-H amine groups [9], [10].
1716.34	H ₂ O	Absorption band corresponding to water molecules adsorbed on nanoparticles [6].
1544.70, 1491.67, 1474.31 and 1435.74	Fe-O Or Fe-OH	Vibration band corresponding to the deformation (bending) of Fe-O or Fe-OH links [6].



Fig. 3 IR spectrum of the synthesized (Fe₃O₄ / CA) composite

2. EFFECT OF CONTACT TIME

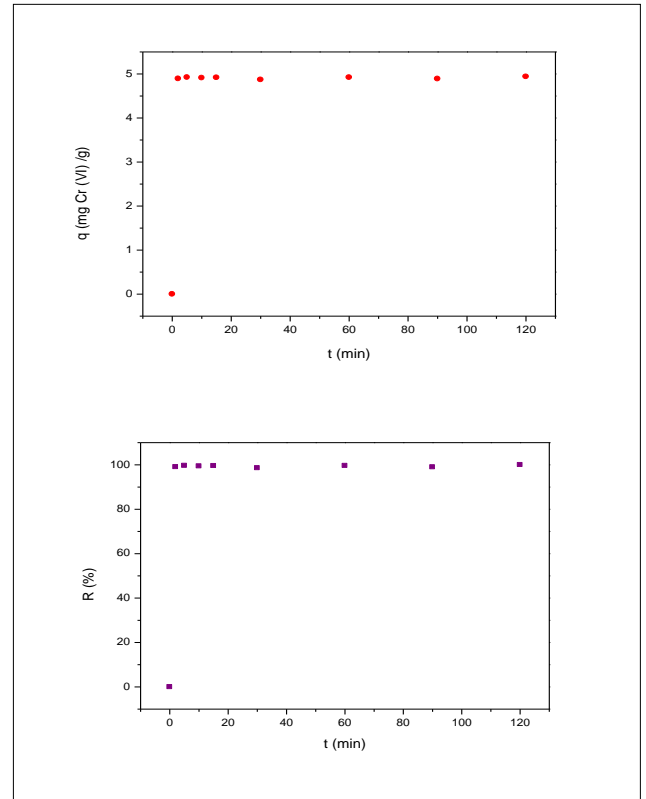


Fig. 4 The Effect of contact time of Cr (VI) by Fh
Conditions : $C_0 = 50$ mg/L, $T = 25^\circ\text{C}$, $d = 0.125\text{mm}$,

$v = 400$ tr/min, r (S/L) = 10 g/L

3. EFFECT OF THE INITIAL CONCENTRATION

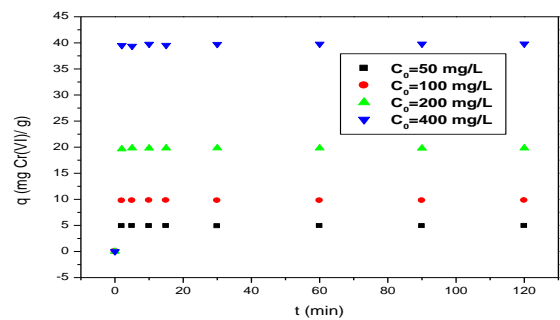


Fig. 5 The effect of initial concentration on Cr (VI) removal by Fh.

Conditions : $T = 25^\circ\text{C}$, $d = 0.125\text{mm}$,

$v = 400$ tr/min, r (S/L) = 10 g/L

4. MODELIZATION

Table 3. Kinetic model

2nd order kinetics	Constants	C ₀ = 50 mg/L	C ₀ = 100 mg/L	C ₀ = 200 mg/L	C ₀ = 400 mg/L
	K ₂ (g. mg ⁻¹ . min ⁻¹)	2.122 24	6.682 26	19.801 98	0.5000 07
	q _e (mg/g)	4.924 41	9.794 32	19.801 98	39.840 64
	R ²	0.999 98	1	1	1

5. ADSORPTION'S ISOTHERMS

Table 4. Different Isotherms of sorption

Types of isotherms	Isotherm's constants		R ²
Langmuir	q _m =40.9157 (mg/g)	K _L =0.64635 (L/mg)	0.9495
Freundlich	K _F =16.3592 (mg.g ⁻¹ (L.mg ⁻¹) ^{1/n})	n= 1.2122 1/n= 0,82495	0.9224
Temkin	b _T =0,2031654 KJ/mol	Ln A _T = 1.7160	0.79519
BET	q _m =13.1788 (mg/g)	K= 850.718	0.46915

IV. DISCUSSION

IV.1. ANALYSIS BY IRTF SPECTROSCOPY

According to Figure 2 and Tables 1 and 2, we observed that when the spectra of the two samples, manufactured ferrihydrite (Fh) (before adsorption) and ferrihydrite loaded with hexavalent chromium (after adsorption), are compared, a shift in practically all peaks is seen, with an increase in the strength of the existing peaks. This shows that functional groups (carboxyl, alcohol, phenol, and amine) are involved in the adsorption of Cr (VI) on Fh.

The IR spectrum of the synthesized composite (Fe₃O₄ / CA) is shown in this figure (Fig. 3) an adsorbed water produces a weak peak at 3423.03 cm⁻¹. While the peaks at 3389.28 cm⁻¹ and 1116.58 cm⁻¹ are caused by stretching and bending vibrations of the O-H bonds, which support the existence of hydroxyl functional groups, respectively (which may be an alcohol, phenol, or carboxyl) [11], [12], [13] and a modest peak at 1116.58 cm⁻¹ indicates the stretching vibration of C-OOH bonds, but the peak at 1330.64 cm⁻¹ in the region (1400–1000 cm⁻¹) indicates the elongation vibration of C-OH bonds, confirming the existence of -COOH groups [14]. Indeed, the elongation vibrations of the C = C and C - C bonds are shown by two peaks at 1625.12 cm⁻¹ and 839.84 cm⁻¹, respectively. At 566.969 cm⁻¹, a wide band of extremely high intensity is tuned to the stretching vibration of Fe - O bonds in the crystal lattice [13].

IV.2. EFFECT OF CONTACT TIME

According to figure 4 (Fig. 4), which represents the variation of the adsorption capacity q as a function of the contact time, we noticed that equilibrium is reached after 15 minutes with an efficiency of 99.511%, indicating the presence of two phases: one rapid and one constant. Also, the speed decreases until 60 minutes have passed, indicating that the sites are saturated.

IV.3. EFFECT OF THE INITIAL CONCENTRATION

In accordance with the figure (Fig. 5), we noticed a proportionality between the retention capacity and the initial concentration of Cr (VI). Indeed, an increase in the amount of pollutant adsorbed on unbound active sites. The maximal retention capacity rises from 4.9163 mg/g for a 50 mg/L starting dosage to 39.8075 mg/g for a 400 mg/L initial concentration.

IV.4. MODELIZATION

According to the recapitulative table (Table 3), we observed that the R^2 numbers for the **pseudo-second-order model** are very satisfactory. It can be inferred that the **pseudo-2nd-order model** better describes the retention kinetics of Cr (VI) by Fh than the other models.

IV.5. ADSORPTION'S ISOTHERMS

When compared to other models (Table 4), the Cr (VI) retention mechanism is best described by a single-layer monolayer isotherm (the Langmuir isotherm) with the greatest correlation factor and the closest to unity (indicating adequate linearization (Langmuir isotherm $q_m = 40.9157$ mg/g)). Indeed, there is no discernible difference between the Freundlich and Langmuir R^2 numbers. We also observe that n between 0 and 10 shows positive adsorption [15], which suggests a rise in Q sorption and the deposition of new adsorbents. The heat constant b_T is positive according to the Temkin isotherm, indicating that the absorption is physical and exothermic [16], [17].

V. CONCLUSION

After this experimental study with the aim of testing our synthesized material prepared in the laboratory (Fh) with respect to water purification. We could conclude that at pH= 3.87, a temperature $T = 25^\circ\text{C}$, a stirring speed $v = 400$ rpm, a grain diameter $d = 0.125$ mm, and a solid/liquid ratio $r(S/L) = 10$ mg/L, **the maximum retention**

capacity is 40.9157 mg / g (The Langmuir isotherm) with a removal efficiency of 99.511% where equilibrium is reached after 15 minutes of contact.

ACKNOWLEDGMENT

The authors are grateful to the Algerian Ministry of higher Education and Scientific Research for financial support.

REFERENCES

- [1] S. Javed *et al.*, "Limited Phosphorous Supply Improved Lipid Content of *Chlorella vulgaris* That Increased Phenol and 2-Chlorophenol Adsorption from Contaminated Water with Acid Treatment," *Processes*, vol. 10, no. 11, 2022, doi: 10.3390/pr10112435.
- [2] R. M. Cornell and U. Schwertmann, *The Iron Oxides : Structure, Properties, Reactions, Occurrences and Uses*, WILEY-VCH. Weinheim, 2003.
- [3] A. Khalfaoui, "Etude Expérimentale de L'élimination de Polluants Organiques et Inorganiques par Adsorption sur des Matériaux Naturels: Application aux Peaux d'Orange et de Banane," thèse en vue de l'obtention du doctorat en sciences en génie des procédés, Université Mentouri, Constantine, 2012.
- [4] S. BELATTAR, "Contribution à l'étude de la dégradation photochimique de polluants organiques par les oxyhydroxydes de Fe (III) en solution aqueuse en phase hétérogène," thèse présentée pour obtenir le diplôme de doctorat en sciences en chimie physique et analytique, Université Mentouri, Constantine, 2018.
- [5] Lise Rancourt, "Adsorption de l'ion arsénate sur des hydroxydes de Fer," Memory presented as a partial requirement for the master's degree in water sciences, University of Quebec Canada, 1993.
- [6] H. LAVERSIN, "Traceurs et formes chimiques du fer dans les particules émises dans l'atmosphère depuis un site sidérurgique : Etude spectroscopique et caractérisation de composés de référence et de particules collectées dans l'environnement.," Thesis to obtain the title of doctor in chemistry, University of Littoral - Côte Opale, 2006.
- [7] H. Tuysuz, E. L. Salabas, C. Weidenthaler, and F. Schuth, "Synthesis and Magnetic Investigation of Ordered Mesoporous Two-Line Ferrihydrite," *J. AM. CHEM. SOC.*, vol. 130, no. 1, pp. 280–287, 2008.
- [8] M. S. Seehra, P. Roy, A. Raman, and A. Manivannan, "Structural investigations of synthetic ferrihydrite nanoparticles doped with Si," *Solid State Commun.*,

- vol. 130, pp. 597–601, 2004, doi: 10.1016/j.ssc.2004.03.022.
- [9] F. ROUESSAC and A. ROUESSAC, *ANALYSE CHIMIQUE : Méthodes et techniques instrumentales modernes*, 6^{eme} éd., Paris, 2004.
- [10] S. Shakoor and A. Nasar, “Utilization of Punica granatum peel as an eco-friendly biosorbent for the removal of methylene blue dye from aqueous solution,” *J. Appl. Biotechnol. Bioeng.*, vol. 5, no. 4, pp. 242–249, 2018, doi: 10.15406/jabb.2018.05.00145.
- [11] M. Bagavathi, A. Ramar, and R. Saraswathi, “Fe₃O₄–carbon black nanocomposite as a highly efficient counter electrode material for dye-sensitized solar cell,” *Ceram. Int.*, pp. 1–33, 2016, doi: 10.1016/j.ceramint.2016.05.111.
- [12] L. Ren, H. Lin, F. Meng, and F. Zhang, “One-step solvothermal synthesis of Fe₃O₄@Carbon composites and their application in removing of Cr (VI) and Congo red,” *Ceram. Int.*, pp. 1–7, 2018, doi: 10.1016/j.ceramint.2018.11.132.
- [13] M. J. Chen, H. Shen, X. Li, and H. F. Liu, “Facile synthesis of oil-soluble Fe₃O₄ nanoparticles based on a phase transfer mechanism,” *Appl. Surf. Sci.*, vol. 307, pp. 306–310, 2014, doi: 10.1016/j.apsusc.2014.04.031.
- [14] J. M. O’Reilly and R. A. Mosher, “Functional groups in carbon black by FTIR spectroscopy,” *Carbon N. Y.*, vol. 21, no. 1, pp. 47–51, 1983, doi: 10.1016/0008-6223(83)90155-0.
- [15] Z. Rawajfih and N. Nsour, “Characteristics of phenol and chlorinated phenols sorption onto surfactant-modified bentonite,” *J. Colloid Interface Sci.*, vol. 298, no. 1, pp. 39–49, 2006, doi: 10.1016/j.jcis.2005.11.063.
- [16] O. Hamdaoui and E. Naffrechoux, “Etude des équilibres et de la cinétique d’adsorption du cuivre Cu(II) sur des particules réactives dans un réacteur fermé, parfaitement agité et thermostaté,” *Leban. Sci. J.*, vol. 6, no. 1, pp. 59–68, 2005.
- [17] N. Fayoud, S. Alami Younssi, S. Tahiri, and A. Albizane, “Etude cinétique et thermodynamique de l’adsorption de bleu de méthylène sur les cendres de bois,” *J. Mater. Environ. Sci.*, vol. 6, no. 11, pp. 3295–3306, 2015.